Progress In Electromagnetics Research C, Vol. 131, 1–12, 2023

Investigation on a Small 4T4R MIMO Microstrip Antenna for Sub-6 GHz New Radio Wireless Network

Satya Singh and Milind Thomas Themalil*

Abstract—The next generation 4T4R Multiple Input Multiple Output (MIMO) antenna solution is gradually accepted by operators in many countries as a mainstream expansion to long term evolution (LTE) networks. Using limited spectrum and high capacity, operators have successfully adopted multi-sector 4T4R MIMO deployment and achieved a 70% increase in capacity without increasing spectrum, thus paving way for state of art next generation wireless networking environment requiring antennae that are robust, small size, lighter, preferably with circular polarization. MIMO antennae provide optimality by arresting multipath fade effect and ensuring data link that is reliable. MIMO realizes efficiency in mobility with the increase in capacity of links and several sub-bandwidths using polarization diversity providing better cyber security. This work therefore is an investigation on a small size 4T4R MIMO antenna for the use in a sub-6 GHz new radio (NR) band in a fading environment with good inter element as well as radiation isolation compared with earlier research. A rectangular patch with loaded slots is designed to obtain small size. Stubs and parasitic elements are introduced between the elements for better mutual coupling performance. Performance of the antenna is stable, with the test results agreeing. The parametrics follow the coefficient of transmission isolation technique to obtain an optimal envelope correlation coefficient (ECC).

1. INTRODUCTION

Future 6G networking is a promising research area of interest in both academics and industries, with nearly hundred times higher access rate than 5G, lower accessing delay, larger communications coverage, better energy efficiency and spectral usage. It enables the technology processes and evolution of antennae and radio frequency systems [1–3]. The Internet of Space is amongst the evolutionary aspects of 6G, needing newer antennae that work in K-bands and above to achieve larger coverage at any given time. The 4T4R 6-sector solution supports cell splitting, and 4×4 MIMO improves spectral efficiency and significantly boosts capacity. MIMO environment offers optimality in cyber security and efficiency. There is a satiating of the popular demand of reliable and speedy communication in multi-media with spectral constraints [4–6].

However, elemental coupling among several antenna elements needs to be overcomed since it affects the parametrics of the MIMO system as a whole. Coupled elements degrade the system by increasing channel losses, decreasing gain, and fading radiation pattern; spatially radiating slots are loaded in the present design to achieve better isolation by using a match between the feeds. A decoupled structure is etched under the feeding elements to overcome coupling, and slots are loaded on the individual patches in the 4T4R structure, thus making a novel design as introduced in this paper and its prototype. Measurements of these small sized MIMO antennae having small ECC, highest diversity and isolations in the network in a faded environment are presented. MIMO antennae take advantage of the multi-path propagation, culminating to multiple propagations characteristic to channels [7, 8]. Upon employing

Received 19 January 2023, Accepted 16 February 2023, Scheduled 6 March 2023
* Corresponding author: Milind Thomas Themalil (milindthomas@gmail.com).
The authors are with the JK Lakshmipat University, India.

MIMO technique, the capacity of faded channel may be variably increased in accordance with Shannon law, thus improving channel throughput [9–11]. As spectral bandwidth is costly, innovations are expected to overcome bandwidth restrictions. High throughput designs have evoked much research enquiry. Reliability between transmitter and receiver as an important basis for performing of a wireless network has received much attention [12–14]. 6G networks require multi-functionality-bands and higher data transfers, while ensuring low costs [15, 16]. Bit error rate (BER) vs signal-to-noise ratio (SNR) is a constant challenge, and efforts are in place for assessing MIMO environment viz-à-viz technique for improvisation [17–19]. Moreover, the authors of this paper have researched the design of MIMO antennae by evaluating BER vs SNR performance [20–22]. With MIMO throughput is increased by no change in power, thus overcoming the challenge of single antenna offering multiplexed diversity gains eradicating the effect of faded channels [23, 24]. Deploying smart antennae has become crucial for optimizing coverage, capacity, and mobility, enabling better service to achieve the fullest potentiality of internet-of-things, the mobile wideband 5G-new-radio allowing reliable concurrent connection at very low latency of lesser than one ms delay [25]. Conventional antennae use metallic rod types, capacitor, etc., making them passive; however, 5G and beyond differ from this design in the sense that they require active antennae, driven as massive (mMIMO) using 16×16, 32×32, and 64×64 configurations to increase throughputs.

MIMO non-arrayed type is used at both sources and destinations for enhanced signal quality and gains since we need compensation for attenuated signal blockage on multi-paths [26]. MIMO smart antennae use beamforming of radio mirror waves focusing radio-frequency energy radiated from the multi-elements in a narrower beam and then transmitting to multi-terminals, as shown in Fig. 1. Such antennae have smart signal processing algorithm used for tracking and locating radiation beams. mmWave communication offers more power to RF signals making fading higher than lower frequencies. Also, mmWave signals have substantial attenuation during propagation due to environmental effects, structures, etc., which require more base stations. Mission criticality applications have popular demands for better voice-data and machine-to-machine communication in the event of disasters or strategic missions [27]. Applications such as robots, driverless vehicles, vehicle-to-anything communication, surgery, drone, or autonomous aerial vehicle do benefit from improvised bandwidth and latency-less features once 5G antennae are deployed [28].

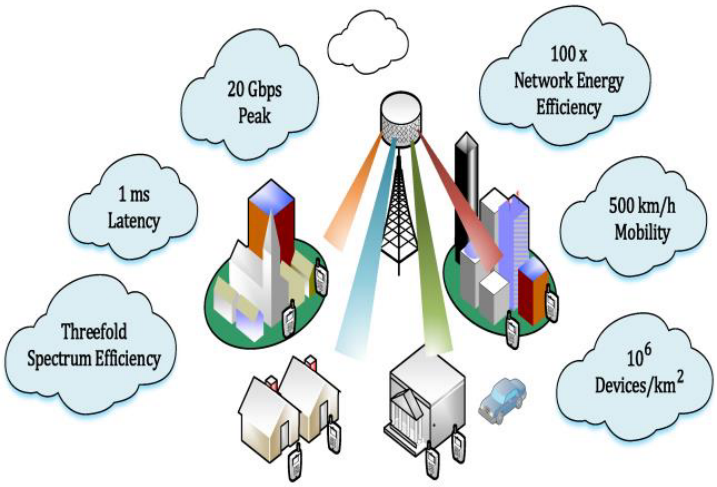

Figure 1. Future 6G MIMO ecosystem.

In spite of researches on 5G antennae system, there are criticalities in designs, including antennae parametrics, integrations, capacity, and spectral efficiency, to ensure reliability and secure communication. Movements of users holding mobile handsets vary stochastically resulting in changes in antenna inclinations leading to multiple paths and fluctuated signal strengths [29]. To overcome these issues, 6G aims to improvise antenna's total efficacy by nearly thirty per cent for larger coverage by more than ninety per cent [30]. Antenna weight is lightly maintained to ensure that installing costs

are reduced. Emerging industry gaps are filled by combining advanced light-weight antennae with 6G communication capabilities [31, 32]. Channel gain that is stronger for user is a choice criterion for antennas selection depending on channel strength. The first antenna transmits to tx-rx chain, and pilot known symbol is sent to base station (BS). The index of antenna at BS switches antenna by user, and second antenna transmit-receive radio chain allows the BS to obtain channel strength.

2. ANTENNA DESIGN AND ANALYSES

Loading slots or slits on the patch elongates its electrical length thus reducing the physical size of the patch, which is the physical principle for achieving compactness or miniaturization in the present design. The antenna in present work is etched on an RT Duroid substrate having dielectric epsilon of $\varepsilon_r = 2.2$, $\tan\delta = 0.00085$, and heighth $= 1.6$ mm, and simulations are done in the range of 2 to 3 GHz, which is an LTE NR sub-6 GHz band as shown in Fig. 2(a). In this design, we have modified a rectangular patch with loaded slots to obtain small size to be compatible with smaller LTE devices. All slots are separated by low characteristic impedance. This antenna is analyzed by incorporating two stages: firstly, the individual load impedance is simulated using integral equations based on reciprocity, with no interaction between the ports. Secondly, a transmission line model is employed where the coupling points are considered as a lumped load.

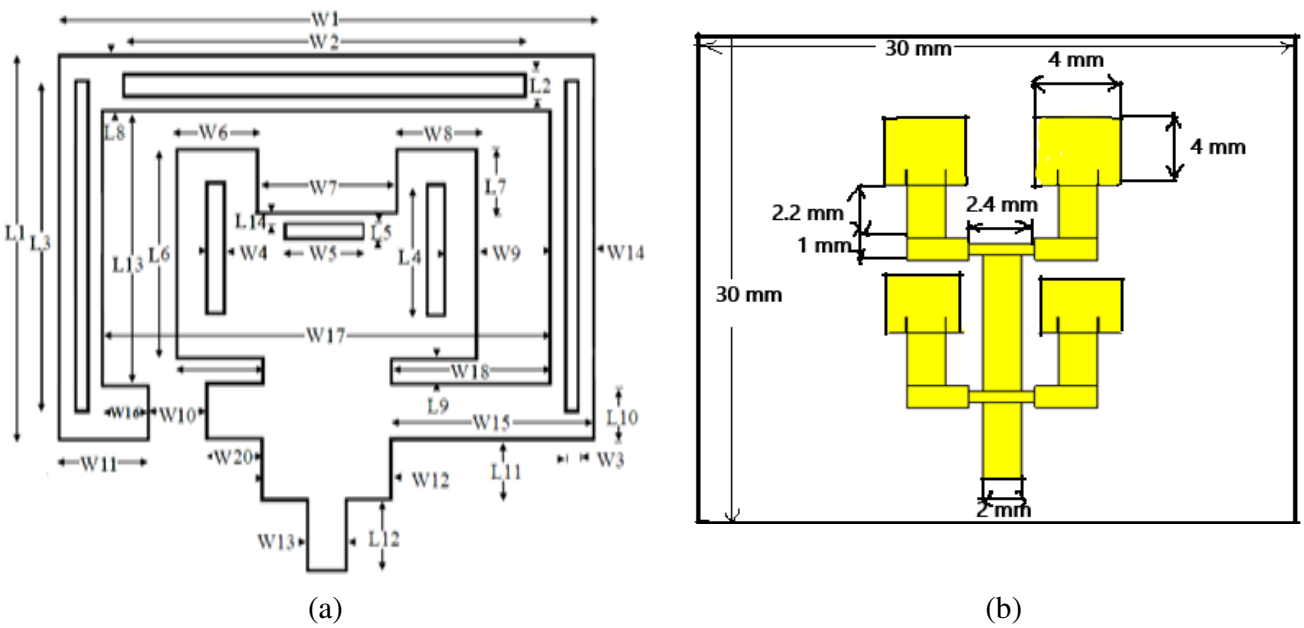

Figure 2. (a) View of single patch of 4T4R antenna. (b) View of 4T4R antenna.

In Fig. 2(a), the dimensions of the individual patch of the later miniaturized into 4T4R antenna as in Fig. 2(b) are tabulated in Table 1 below.

The miniaturized 4T4R system is shown in Fig. 2(b). The steps to calculate the dimensions are given below [9].

Step 1: Width estimation

$$W = \frac{1}{2f_r\sqrt{\mu_0\varepsilon_0}}\sqrt{\frac{2}{\varepsilon_r+1}} = \frac{v_0}{2f_r}\sqrt{\frac{2}{\varepsilon_r+1}} \tag{1}$$

Step 2: Effective permittivity constant estimation is based on the height, dielectric permittivity of the substrate, and the estimated width of the squares.

$$\varepsilon_{reff} = \frac{\varepsilon_r+1}{2} + \frac{\varepsilon_r-1}{2}\left[1+12\,\frac{h}{W}\right]^{-1/2} \tag{2}$$

Step 3: Electrical length extension ΔL

$$\frac{W}{h} > 1$$

$$\frac{\Delta L}{h} = 0.412 \frac{(\varepsilon_{reff} + 0.3)\left(\frac{W}{h} + 0.264\right)}{(\varepsilon_{reff} - 0.258)\left(\frac{W}{h} + 0.8\right)} \tag{3}$$

Step 4: Physical effective length

$$L_{eff} = \frac{1}{2f_r\sqrt{\varepsilon_{reff}}\sqrt{\mu_0\varepsilon_0}} \tag{4}$$

Step 5: Total real length of the patch

$$L = L_{eff} - 2\Delta L \tag{5}$$

where f_r is the centre frequency, W the patch's width, L is the patch's length, h the substrate's height, and ε_r the substrate's permittivity. TM_{010} mode and the centre frequency of the antenna related to its length are expressed as

$$(f_r)_{010} = \frac{1}{2L\sqrt{\varepsilon_r}\sqrt{\mu_0\varepsilon_0}} = \frac{v_0}{2L\sqrt{\varepsilon_r}} \tag{6}$$

In the presented design of antenna structure, stubs are printed on the ground-plane improving the isolation. To lower the insertion loss, parasitic elements are also etched. A coupling field is created which oppose the primary field so as to minimize the total insertion losses. Antenna is fabricated using photolithography as in Fig. 3.

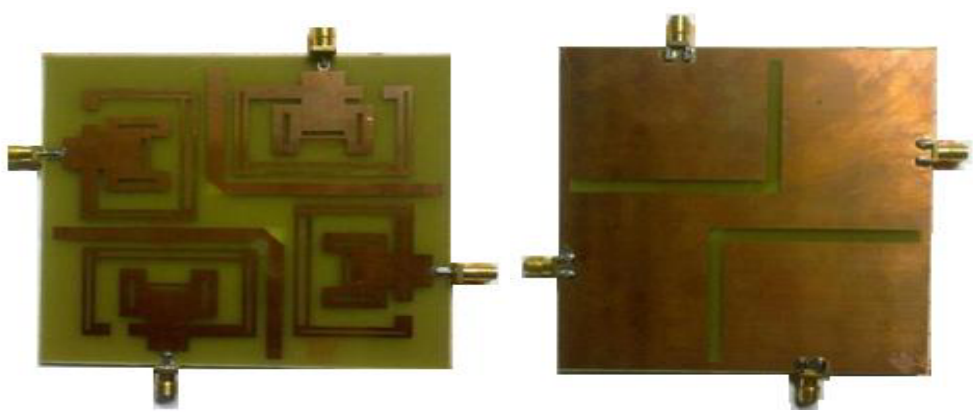

(a) (b)

Figure 3. (a) Frontal view of fabricated MIMO antenna Fig. 3. (b) Fabricated ground plane.

Figure 4 depicts the equivalence of the printed antenna of the 4T4R MIMO patch. The decoupled components are modeled as LL and CR. The antennae are modeled as a cascading resonance sequence.

To calculate L, length, and W, width of the patches, the following equations are employed [9]

$$Ws = 6h + Wp \tag{7}$$

$$Ls = 6h + Lp \tag{8}$$

Equations (1) to (8) are employed to determine the dimensions of the overall antenna, and thereafter optimization of lengths and widths of overall patch as well as slots and ground plane are performed using CST software by parametric optimization for each variable indicated in Table 1.

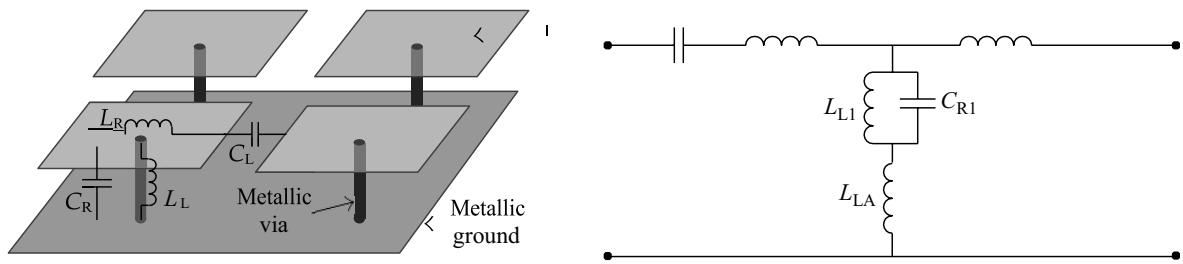

Figure 4. Circuit equivalence of prototype.

Table 1. Parametrics of the antenna.

Length (mm)		Width (mm)	
$L1$	28.2	$W1$	42.4
$L2$	2	$W2$	35
$L3$	25	$W3$	1
$L4$	10	$W4$	1.5
$L5$	1.5	$W5$	10
$L6$	15.5	$W6$	6.3
$L7$	4.6	$W7$	11.2
$L8$	4	$W8$	6.3
$L9$	1.9	$W9$	2.4
$L10$	4	$W10$	4.6
$L11$	4.5	$W11$	7
$L12$	5	$W12$	10.2
$L13$	0.1	$W13$	2.8
$L14$	0.9	$W14$	4
Center Frequency	2.55 GHz	$W15$	16.1
		$W16$	3.6
		$W17$	35.7
Bandwidth	100 MHz	$W18$	12.7
		$W19$	6.8
		$W20$	4.4

3. TRANSMISSION COEFFICIENT METHOD

ECC is an industry standard radiation pattern correlation metric, which indicates how independently two antennae radiate, e.g., if one antenna is fully horizontally polarized and the other fully vertically polarized, the two antennae have zero correlation. Hence, ECC considers the antenna radiation pattern shape, polarization, and the relative phases of the field. If antennae produce high correlated field patterns, they will also produce low isolation due to reciprocity. In the present work, the transmission coefficient method to optimally estimate the ECC is used, which is a pattern related parametric, so that the antennae have sufficient isolation by having each respective radiation pattern independently thus providing simultaneous transmissions. MIMO antennae require high ECC to have optimal efficiency [28].

The mathematical expression used for fields F_1 and F_2 is given by

$$\rho_e = \frac{\left| \iint \overline{F_1} \cdot \overline{F_2^*} d\Omega \right|^2}{\iint \left|\overline{F_1}\right|^2 d\Omega \cdot \iint \left|\overline{F_2}\right|^2 d\Omega} \tag{9}$$

If F_1 and F_2 are the same, then ECC is 1; otherwise, it is nil, implying independent non-correlated fields. The expression for ECC as isolation S_{12} or S_{21} and return loss S_{11} is

$$\rho_e = \frac{\left|S_{11}^* S_{12} + S_{21}^* S_{22}\right|^2}{\left(1 - |S_{11}|^2 - |S_{21}|^2\right)\left(1 - |S_{22}|^2 - |S_{12}|^2\right)} \tag{10}$$

ECC is optimized through transmission coefficient S_{12} isolation parameter, which is the industry factor for estimating MIMO antenna performance. ECC < 0.2 covers the operational sub-6 GHz frequency in the present work. ECC can also be estimated using S-parameter of radiated far-fields [20–25]. The spectral efficiency η max relates the total efficiency correlated by all antennae [25], mentioned by Equation (11) below where $\eta 1$ and $\eta 2$ are efficiencies of any two antennae.

$$\eta \max = \sqrt{\eta 1 \eta 2 (1 - \mathrm{ECC})} \tag{11}$$

4. RESULTS AND DISCUSSION

The measured results of the present 4T4R antenna design are validated through measurements using VNA wherein one port is 50 ohm matched, and output is obtained from other port after calibration. The measured S-parameters are in Fig. 5.

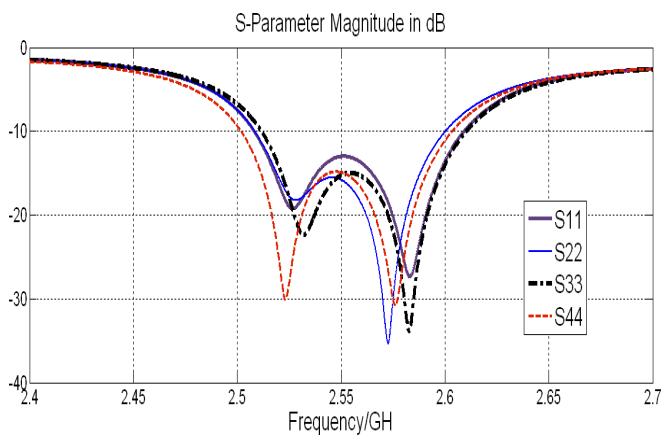

Figure 5. Return loss of MIMO antenna.

As in Fig. 5, measured results agree with the computational ones. All four fed ports are aligned at centre frequency of 2.55 GHz with good matching; S_{11}, S_{22}, S_{33}, and S_{44} are below -10 dB. The -10 dB return-loss-bandwidth between 2.5 and 2.6 GHz is 100 MHz sufficient in the sub-6-GHz NR band requirements.

Figure 6 depicts the 2 : 1 voltage standing wave ratio (VSWR) bandwidth is also 100 MHz between 2.5 and 2.6 GHz; however, a 25 MHz shift between the measured and simulated results is because of the effects of dielectric constant, substrate thickness, and solder joints of SMA. Acceptable 2 : 1 VSWR value ensures less power reflection to source than the case wherein there is no proper impedance matching to 50 ohms. The insertion loss within 2.5 to 2.6 GHz operating band is below -25 dB; insignificantly small energy is coupled from port 1 to 2, port 1 to 3, and port 1 to 4, respectively. Decoupled antenna structure allows nil current from port 1 to 2, port 3 to 4; sufficiently isolated below -25 dB is obtained within 2.5 to 2.6 GHz range, as shown in Fig. 7. A small difference between measured and simulated

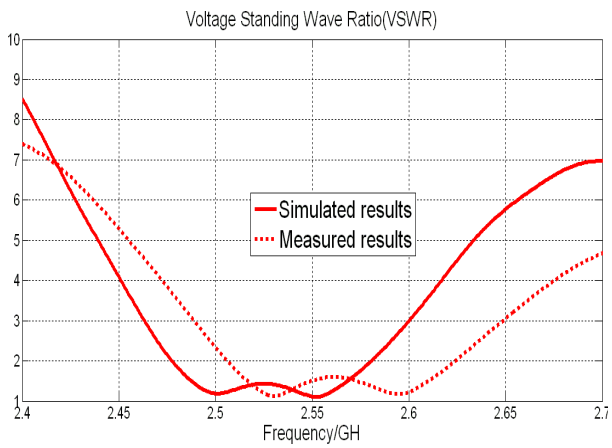

Figure 6. Measured VSWR of the antenna.

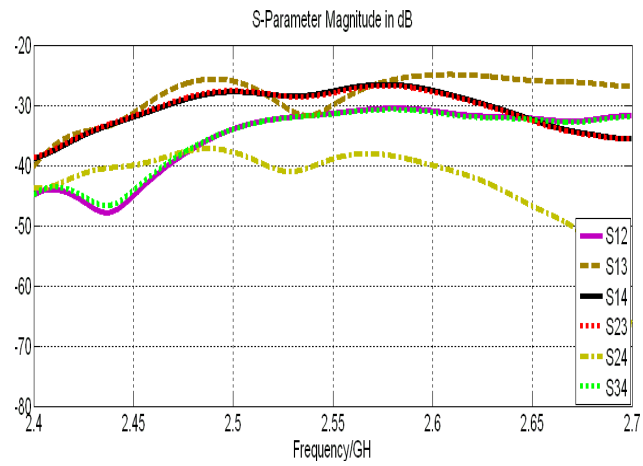

Figure 7. Measured insertion losses.

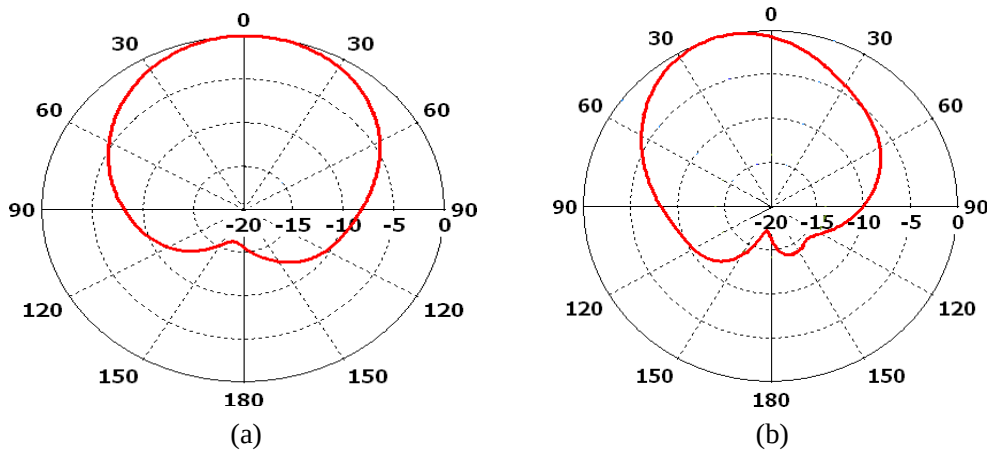

Figure 8. Pattern at 2.55 GHz, (a) for $\Phi = 0°$, (b) for $\Phi = 90°$.

values is due to varying thickness of dielectrics in available substrates in market. Impedance mismatch, solder joints, and misalignment also play a role. It can be seen that the bandwidth of the fabricated antenna is smaller due to parasite elements.

Figure 8 depicts the measured radiation patterns, estimated at fixed distance and frequency, at $\Phi = 0°$ and $\Phi = 90°$ for the fabricated antenna at centre frequency $f_r = 2.55$ GHz, producing directional pattern. The main beam angle is about broadside direction. The E-plane directionality is tilted onto the right side at 2.55 GHz due to the effect of parasitic elements. Directional radiated pattern tilted left in H-plane can be seen. The main beam angle is about broadside direction with a beamwidth of 108°. The back radiation is significantly smaller. Lower back radiation is an important reason for using the antenna in cell phones since there is reduction in amount of radiation towards the users head. The far field directivities at Phi = 0° and Phi = 90° are shown in Fig. 9.

Measured gain, directivity, and half-power bandwidth (HPBW) are compared in Table 2 below.

Diversity behavior of the MIMO antenna is estimated using ECC method. The radiation patterns of antennae are orthogonally polarized, where each patch is rotated 90° with reference to the other. Polarization diversity method improves capacity with smaller spacing between antennae.

The present 4T4R planar MIMO patch antenna provides very small correlation below 0.02 in the desired frequency band from 2.5 to 2.6 GHz as shown in Fig. 10. This is due to excellent isolation and lower coupling among the four antennae. The correlation coefficient is measured for port 1:2,

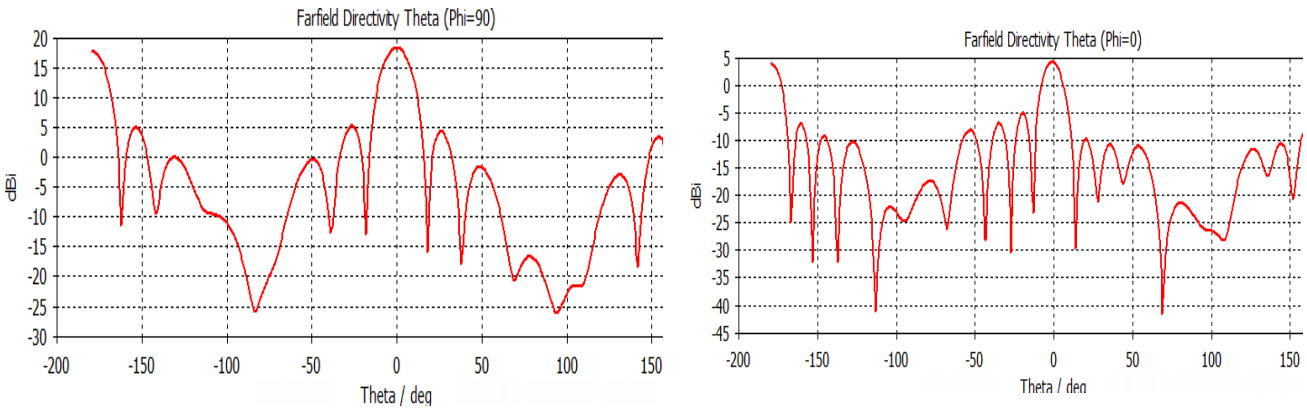

Figure 9. Far-field directivities at Phi = 0° and Phi = 90°.

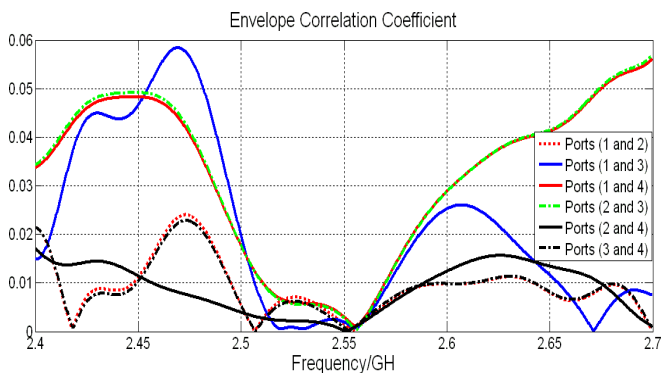

Figure 10. ECC reading of antenna.

Table 2. Comparing simulated and measured values.

Parameter	Simulated	Measured
Gain	3 dB	2.5 dB
Directivity	5 dB	4.2 dB
HPBW	110°	108°

port 1:3, port 1:4, port 2:3, port 2:4, and port 3:4, respectively, thus obtaining desired diversity. The simulated and measured axial ratios vs frequency values are shown in Table 3 below. Fig. 11 shows the corresponding plots of simulated and measured axial ratios vs frequency values. Good axial ratio of 0.4 dB is obtained around the centre frequency between 2.4 and 2.8 GHz band offering desirable circular polarization, provided by the perpendicularly loaded slot arrangement on the patch.

5. COMPARATIVE RESULTS AND COMMENTS

The challenges posed by earlier researches [19] due to physical influence of dimension of substrate and multiple components were studied. Return loss is maintained in the present work that is below −15 dB at frequency 2.55 GHz. The efficiency of the antenna is improved from 8% to 9% with no compromise on the mutual coupling at centre frequency, because usually while optimizing efficiency there is more mutual coupling which can bring down the isolation thus increasing ECC, not desirable in MIMO, so we use decoupled components (LL and CR), as shown in Fig. 4 earlier, to mitigate this effect. In the current

work, gain has been improved from 2.2 dBi to 2.5 dBi. The dimensions of the antenna get miniaturized to 15% compared to earlier designs [10–16].

4T4R MIMO antenna is enhanced by LTE uplink using diversity schemes. Similarly, 2×2 MIMO

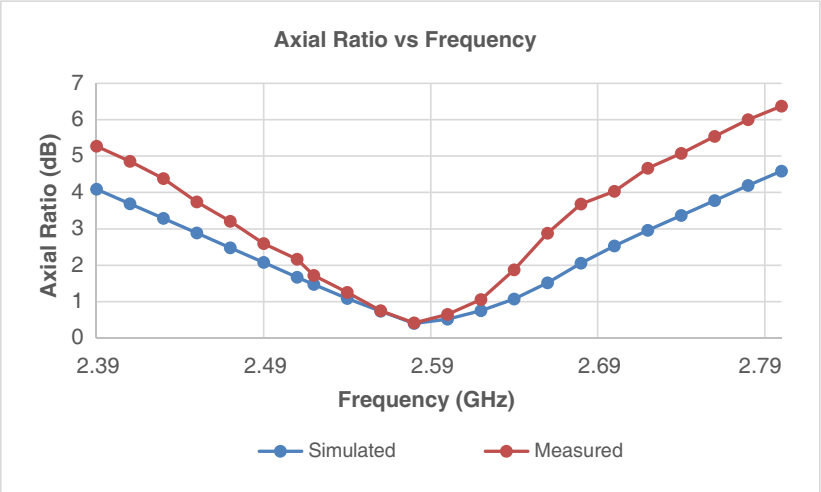

Figure 11. Plot of simulated vs measured axial ratio vs frequency.

Table 3. Simulated vs measured axial ratio values.

Frequency	Simulated	Measured
2.39	4.09	5.275
2.41	3.69	4.856
2.43	3.29	4.384
2.45	2.89	3.739
2.47	2.48	3.207
2.49	2.08	2.595
2.51	1.67	2.166
2.52	1.47	1.718
2.54	1.09	1.255
2.56	0.74	0.752
2.58	0.41	0.414
2.6	0.52	0.651
2.62	0.75	1.061
2.64	1.07	1.876
2.66	1.52	2.881
2.68	2.06	3.683
2.7	2.53	4.032
2.72	2.96	4.668
2.74	3.37	5.078
2.76	3.78	5.539
2.78	4.19	5.999
2.8	4.59	6.375

array, metallic structures are placed between antennae which is a method for providing excellent isolation between elements. The antenna designs [17, 18] for 5G applications show better performance than traditional arrays. Antenna bandwidth is increased by 60% and gain by 6% compared with traditional arrays. The slotted ground structure [19, 20] with single patch antennae shows good performance parameters. Table 4 below shows comparative parametrics of present work.

Table 4. Comparing present antenna to few existing antennae.

Antennae	Bandwidths (MHz)	3 dB-Axial ratio-BW (%)	Axial Ratios (dB)	Directivitys (dBi)	VSWRs	Gains (dB)
[7]	43	3.47%	*1.26*	-	-	0.62
[9]	16	0.65%	*0.97*	-	1.16	-
[10]	187	4.3%	0.65	-	-	7.2
[12]	37	0.54%	*1.03*	-	-	8.49
[14]	-	0.6%	1.11	-	1.22	-
[16]	23	0.99%	*0.20*	-	-	10.8
[18]	66	-	0.64	-	-	8.22
[19]	89	6.5%	*0.96*	-	-	6.2
[20]	116	10.5%	*0.95*	-	1.14	8.05
Proposed antenna	40	1.6%	0.4	10	1.02	2.5

6. CONCLUSION

Current work presents a small 4T4R MIMO antenna with suppressed surface waves. Better isolation using slotted ground is obtained by exploiting the spatial and polarization diversity with enhanced isolation, achieved by etching slotted ground plane with no increase in the previous dimensions of the 4T4R antenna. The measured results agree well with computational ones, confirming the present antenna as an ideal consideration for MIMO ecosystem. The current antennae have slot loaded patches such that the designed antenna radiates at orthogonal patterns.

Good return loss below -15 dB, mutual coupling below -20 dB, and desired bandwidth of 100 MHz are achieved, matched to $50\,\Omega$ in the frequency range covering LTENR band of 2.5 to 2.6 GHz. It is observed that better designs imply better trade-offs among return and insertion losses. As a future work, insertion-loss can be improvised by introducing partial square type strips. Deviations in measurement results from simulated ones are due to the material losses, probe solder joints, spurious radiation from feeds, etc. Bandwidth requirements of the antenna can be enhanced by supporting TM_{10} mode and anti-phase TM_{20} mode simultaneously. As a future work 8×8 and 16×16 size MIMO arrays are being considered for parametric study and simulation.

ACKNOWLEDGMENT

Thanks to IET, JK Lakshmipat University, Jaipur and XLIM, University of Limoges, France.

REFERENCES

1. Ngo, H. Q., "MIMO: Fundamentals and system designs," PhD Thesis, Department of Elect. Engg., Linköping University, Sweden, Sept. 2015.

2. Dohler, M., S. McLaughlin, D. Laurenson, M. Beach, C. M. Tan, and A. H. Aghvami, "MIMO channel measurement and modeling," *IEEE Communications Magazine*, Vol. 45, No. 3, 85–92, Dec. 2007.
3. Dohler, M., S. McLaughlin, and A. H. Aghvami, "Implementable access for MIMO receiver architectures," *IEEE Communications Magazine*, Vol. 45, No. 3, 93–97, Dec. 2007.
4. Björnson, E., J. Hoydis, and L. Sanguinetti, "MIMO networks: Energy and hardware efficiency," *Trends in Signal Processing*, Vol. 11, Nos. 3–4, 154–655, Jun. 2017.
5. Lathi, B. P. and Z. Ding, *Digital Communications*, ISBN 978-0-19-538493-2, 4/e, 2010.
6. De Lamare, R. C., "MIMO systems: Signal processing challenges and future trends," *IEEE Trans. Veh. Technol.*, Vol. 60, No. 6, 2482–2494, Jul. 2011.
7. Lee, W. C. Y., *Mobile Communications Design Fundamentals*, ISBN: 978-0-471-57446-0, Wiley 2/e, 1993.
8. Srivastava, S., A. Gupta, S. Singh, and M. T. Themalil, "Characterization and analysis of bit error rate in binary phase shift keying for future 5G MIMO environment," *Int'l Conference on Innovation and Sustainability (ICIS'21)*, JK Lakshmipat University, Jaipur, Feb. 2021.
9. Balanis, C. A., *Antenna Theory: Analysis and Design*, John Wiley and Sons, Hoboken, New Jersey, May 2005.
10. Waterhouse, R. B., *Microstrip Patch Antennas: A Designer's Guide*, Kluwer Academic, New York, Feb. 2003.
11. Ibrahim, M. S., "MIMO antenna at Ka-band for fifth generation applications," *International Journal of Communication Antennas and Propagation*, Vol. 9, No. 2, 100–109, Apr. 2019.
12. Björnson, E., J. Hoydis, and L. Sanguinetti, "Massive MIMO," *Transactions Wireless Communications*, Vol. 17, No. 1, 574–590, Jan. 2018.
13. Strategic roadmap towards 5G for Europe: RSPG on 5G networks, *Radio Spectrum Policy Group 18-005*, Jan. 2018.
14. Agiwal, M., A. Roy, and N. Saxena, "5G wireless networks survey," *IEEE Communications Surveys*, Vol. 18, 1617–1655, Sept. 2016.
15. Parkvall, S., E. Dahlman, A. Furuskar, and M. Frenne, "5G radio access technology," *IEEE Communications Standards Magazine*, Vol. 1, No. 4, 24–30, Dec. 2017.
16. Patzold, M., "5G readiness," *IEEE Vehicular Technology Magazine*, Vol. 13, No. 1, 6–13, Mar. 2018.
17. Sarkar, D. and K. V. Srivastava, "SRR loaded dual-band MIMO antenna for WLAN/WiMAX/WiFi/4G-LTE and 5G applications," *Electronics Letters*, Vol. 53, No. 25, 1623–1624, Jan. 2017.
18. Jensen, M. and J. Wallace, "Antennas and propagation for MIMO wireless communications," *IEEE Transactions on Antennas and Propagation*, Vol. 52, No. 11, 2810–2824, May 2004.
19. Sharawi, M. S., A. B. Numan, M. U. Khan, and D. N. Aloi, "MIMO antenna system with enhanced isolation for mobile terminals," *IEEE Antennas and Wireless Propagation Letters*, Vol. 11, 1006–1009, Oct. 2012.
20. Cui, L., J. Guo, Y. Liu, and C.-Y.-D. Sim, "An 8-element dualband MIMO antenna with decoupling stub for 5G smartphone applications," *IEEE Antennas and Wireless Propagation Letters*, Vol. 18, No. 10, 2095–2099, Jun. 2019.
21. Stutzman, W. S. and G. A. Thiele, *Antenna Theory and Design*, John Wiley and Sons, 2009.
22. Nossek, J. A. and M. T. Ivrlac, "The why and how of multiantenna systems," *International Workshop on Smart Antennas*, IEEE Xplore: DOI-978-1-4244-1757-5/08, Feb. 2008.
23. Garg, R., P. Bhartia, I. J. Bahl, and A. Ittipiboon, *Microstrip Antenna Design Handbook*, Artech House, 2001.
24. Roy, J. S. and M. Thomas, "Compact broadband microstrip antennas next generation wireless communication HIPERLAN/2," *Intl. Jnl. of Microwave Science and Technology*, Vol. 2007, No. 10, 1–4, Jul. 2007.
25. Roy, J. S. and M. Thomas, "Investigations on a new proximity coupled dual frequency microstrip antenna," *Microwave Review*, Vol. 13, 12–15, Jun. 2007.

26. Roy, J. S., M. Thomas, and J. Ghosh, "Miniaturized broadband circularly polarized microstrip antenna for WLAN," *International Journal of Microwave and Optical Technology*, Vol. 3, No. 4, 467–473, Sept. 2008.
27. Roy, J. and M. T. Themalil, "Design of a circularly polarized microstrip antenna for WLAN," *Progress In Electromagnetics Research M*, Vol. 3, 79–90, 2008.
28. Thomas, M., J. S. Roy, and B. Gupta, "Design of a miniaturized proximity-coupled microstrip antenna for 5 GHz band wireless communication," *ACTA Technica Journal*, Vol. 55, No. 2, 131–138, Apr.–Jun. 2010.
29. Thomas, M., J. S. Roy, and B. Gupta, "Design of circularly polarized T-stub coupled microstrip antenna for WLAN," *Asian Jnl. of Applied Sc.*, Vol. 4, No. 4, 883–888, Aug. 2016.
30. James, J. M. and M. T. Themalil, "Design of heterogeneous wireless mesh network for LTE," *Journal of Computer Sci. and Tech.: E Network, Web Security*, Vol. 17, No. 3, USA, Online ISSN: 0975-4172, Print ISSN: 0975-4350, 2017.
31. Themalil, M. T., S. Singh, D. Jain, D. Yadav, M. Rammal, and M. Sharma, "Miniaturization capability of pixel antenna for nanosatellite footprints," *VLSI, Microwave and Wireless Technologies*, Vol. 877, Lect. Notes Elec. Eng., Springer, ISBN: 978-981-19-0311-3, doi: 10.1007/978-981-19-0312-0, Mar. 20–21, 2021.
32. Singh, S. and M. T. Themalil, "Investigations on 2T2R MIMO microstrip patch antenna for next generation wireless networks," *International Journal of Microwave and Optical Technology*, Vol. 17, No. 6, 630–638, USA, Nov. 2022.